

# **Biosynthesis of Au–Ag Alloy Nanoparticles for Sensitive Electrochemical Determination of Paracetamol**

*Ruisong Wei*

Hechi University, No.42 Longjiang Rd, Yizhou, Hechi, Guangxi, 546300, P.R. China  
E-mail: [ruisongwei\\_eric@foxmail.com](mailto:ruisongwei_eric@foxmail.com)

*Received: 3 June 2017 / Accepted: 3 August 2017 / Published: 12 September 2017*

---

This study reports the bio-preparation of Au–Ag alloy nanoparticles using yeast cells, along with their application in preparing a sensitive electrochemical paracetamol sensor. The sensitive electrochemical detection of paracetamol was performed using a glassy carbon electrode (GCE) after modification of the cellulose diacetate (CDA)/Au–AgNP nanocomposite. The results of cyclic voltammetry (CV) analysis showed the remarkable capacity of CDA/Au–AgNPs to enhance the electrochemical response to paracetamol, which was ascribed to their desirable electronic features. The parameters were studied and optimized. The amperometric oxidation currents in response to paracetamol, recorded under optimal conditions, were found to be linearly proportional to the concentration (0.01 - 0.1 mM). Limit of detection (LOD): 2.6  $\mu$ M (S/N = 3).

---

**Keywords:** Au–Ag alloy; Cellulose diacetate; Paracetamol; Electrochemical determination; Biosynthesis

## **1. INTRODUCTION**

Due to their advantages over monometallic candidates, alloy nanoparticles have attracted substantial attention [1-6]. To be specific, gold–silver (Au–Ag) alloy nanoparticles have the potential to be applied in biomedical fields due to their distinctive structural and electronic features. However, large numbers of alloy nanoparticle preparation techniques have been considered to pose environmental risks [7-10]. Therefore, green strategies for preparing alloy nanoparticles need to be proposed. In recent years, a new technique, the biological system, has been reported for the preparation of different inorganic materials at an exquisite level of complexity [11-13]. In fact, several studies have proposed the application of biological systems for alloy nanoparticle preparation [14-16]. However, the biological systems in these studies are not easy to establish. In addition, the operation requires

extensive time. When metal nanoparticles are introduced into the sensing interface of electrochemical sensors, an electron shift can be promoted, leading to marked enhancement in the sensitivity of the electrochemical sensors [17, 18]. To be specific, compared with other monometallic candidates, bimetallic compositions are more desirable in terms of catalytic selectivity, catalytic activity, and other properties. [19, 20]. To date, Au–Ag [21], Au–Pt [22], Pt–Ni [23], Pt–Pb [24] and Cu–Pd [25] have been proposed for the development of electrochemical sensors. Au–Ag alloy nanoparticles are excellently catalytic and miscible and thus have attracted substantial attention compared with bimetallic nanoparticles [26].

As an effective analgesic and antipyretic drug, paracetamol (acetaminophen, *N*-acetyl-*p*-aminophenol) has been accepted as a desirable substitute for aspirin and has been extensively used for pain and fever relief [27, 28]. Though paracetamol is not prone to addictivity with long-term use and does not cause any side effects when the therapeutic dose is appropriate [29], toxic metabolites accumulate and result in damage to the kidney and liver in the case of paracetamol overdose [30, 31]. Therefore, the proposal of a precise, sensitive, fast, cost-effective, and facile detection strategy was essential for the benefit of the general public health. In recent years, spectrophotometry [32], spectrofluorometry [33], high-performance liquid chromatography [34], titrimetry [35], chemiluminescence [36], gas chromatography [37], capillary electrophoresis [38], electrochemical methods [27, 39-44] and some other analytical strategies have been reported for paracetamol detection. The electrochemical strategy is rapid in response, simple in sample preparation, and low in LOD, and thus, it is more widely accepted than other techniques.

In this report, the synthesis of Au–Ag alloy nanoparticles (NPs) was performed using a new and facile strategy based on easily obtained yeast cells. In addition, the obtained Au–Ag alloy nanoparticles (NPs) were investigated using X-ray photoelectron spectroscopy (XPS) and UV–vis spectroscopy (UVS). In addition, as a sensor for paracetamol, the Au–Ag alloy NPs were immobilized on a GCE surface via CDA, to obtain a CDA/Au–Ag alloy NP hybrid. Then, this hybrid was used to prepare a CDA/Au–AgNP-modified GCE. The as-prepared electrode showed a highly sensitive electrochemical response to paracetamol oxidation. In this study, a sensitive electrochemical sensor for paracetamol detection was prepared based on the Au–Ag alloy NPs formed using a new green strategy.

## 2. EXPERIMENTS

### 2.1. Chemicals

AgNO<sub>3</sub> and aurichlorohydric acid (HAuCl<sub>4</sub>·4H<sub>2</sub>O) purchased from Shanghai Chemical Reagents Co. (Shanghai, China) were dissolved in double-distilled water to obtain concentrations of 10.0 mg/mL and 20.0 mg/mL, respectively. Instant dry yeast was commercially available from Angel Yeast Co. (Yichang, China). Paracetamol, CDA, and sucrose were commercially available from Shanghai Reagent Company. The obtained CDA was dissolved in acetone (1.0 mg/mL) for further use. A stock solution of 0.01 M vanillin was obtained by dissolving in double-distilled water and stored at a temperature of 4 °C. Vanilla tea and vanilla beans were commercially available in a local supermarket.

Other chemicals were of analytical reagent grade and used without further purification. Double-distilled water was used to prepare the aqueous solutions.

## 2.2. Fabrication of colloidal Au–Ag alloy NPs

The following procedure described the synthesis of Au–Ag alloy NPs. The culture medium was synthesized by boiling and then cooling 40 mL of the sucrose solution (50 mg/mL) to 30 °C. The as-prepared solution was mixed with instant dry yeast (600 mg), then maintained at 30 °C for 24 h and centrifuged for 3 min at 2500 rpm to obtain the yeast cells. This step was followed by washing three times using sterile water and then re-suspension in sterile water ( $10^6$  cells/mL). Then, the concentration of the as-prepared yeast cell solution was adjusted to 1.0 mg/mL by adding  $\text{AgNO}_3$  solution and  $\text{HAuCl}_4$  solution at appropriate volumes. The Au–Ag alloy NPs were obtained in the colloidal form by further sealing the as-prepared mixture and keeping it below 30 °C for 24 h.

## 2.3. Preparation of paracetamol sensor

Initially, a GCE was polished using alumina slurry (0.05  $\mu\text{m}$ ), followed by sonication in nitric acid (1:1), ethanol and double-distilled water for 60 s each in turn. Then, the bare GCE was modified using 10  $\mu\text{L}$  of Au–Ag alloy NPs (1.0 mg/mL) in colloidal form and left to dry at room temperature. Five microliters of CDA solution (1.0 mg/mL) was cast onto the Au–AgNPs/GCE surface and then air dried to form a thin CDA film on the modified GCE for the immobilization of the Au–Ag alloy NPs, as it was easy for the Au–Ag alloy NP film to peel off in solution. Then, the final electrode, CDA/Au–AgNP/GCE, was produced and utilized as an electrochemical sensor for paracetamol.

## 2.4. Characterizations

A CHI 660A electrochemical analyser (Shanghai Chenhua Co., China) with a traditional triple-electrode configuration was used for all electrochemical tests. The working, reference, and counter electrode were a GCE modified by a CDA/Au–Ag alloy NP composite film, a saturated calomel electrode, and a platinum wire. Energy dispersive X-ray spectroscopy (EDX, Vantage 4105, NORAN) was used for the elemental composition measurement. XPS analysis was performed on a VG Micro-Tech ESCA 3000 spectrometer, and a multichanneltron hemispherical electron energy analyser was used (pressure: equal to or lower than  $1 \times 10^{-9}$  Torr).

## 3. RESULTS AND DISCUSSION

As indicated in the EDX measurement of the Au–Ag NPs present on the GCE (Fig. 1A), Ag, C and Au were the major elements on the electrode surface, suggesting the coexistence of Ag and Au in the proposed specimen. Au–Ag alloy NP suspensions produced with varying reaction times were

characterized via their UV–Vis absorption spectra, as shown in Fig. 1B. A gradual increase in the absorption peaks (541 - 445 nm) was observed with the prolongation of reaction time, which corresponded to an increase in the Ag mole fraction. Note that only one absorption peak appeared, and all the observed peaks ranged from 545 nm to 413 nm. It can be concluded that Au–Ag alloy NPs are formed rather than either a segregated metal or core/shell-type structure [45].

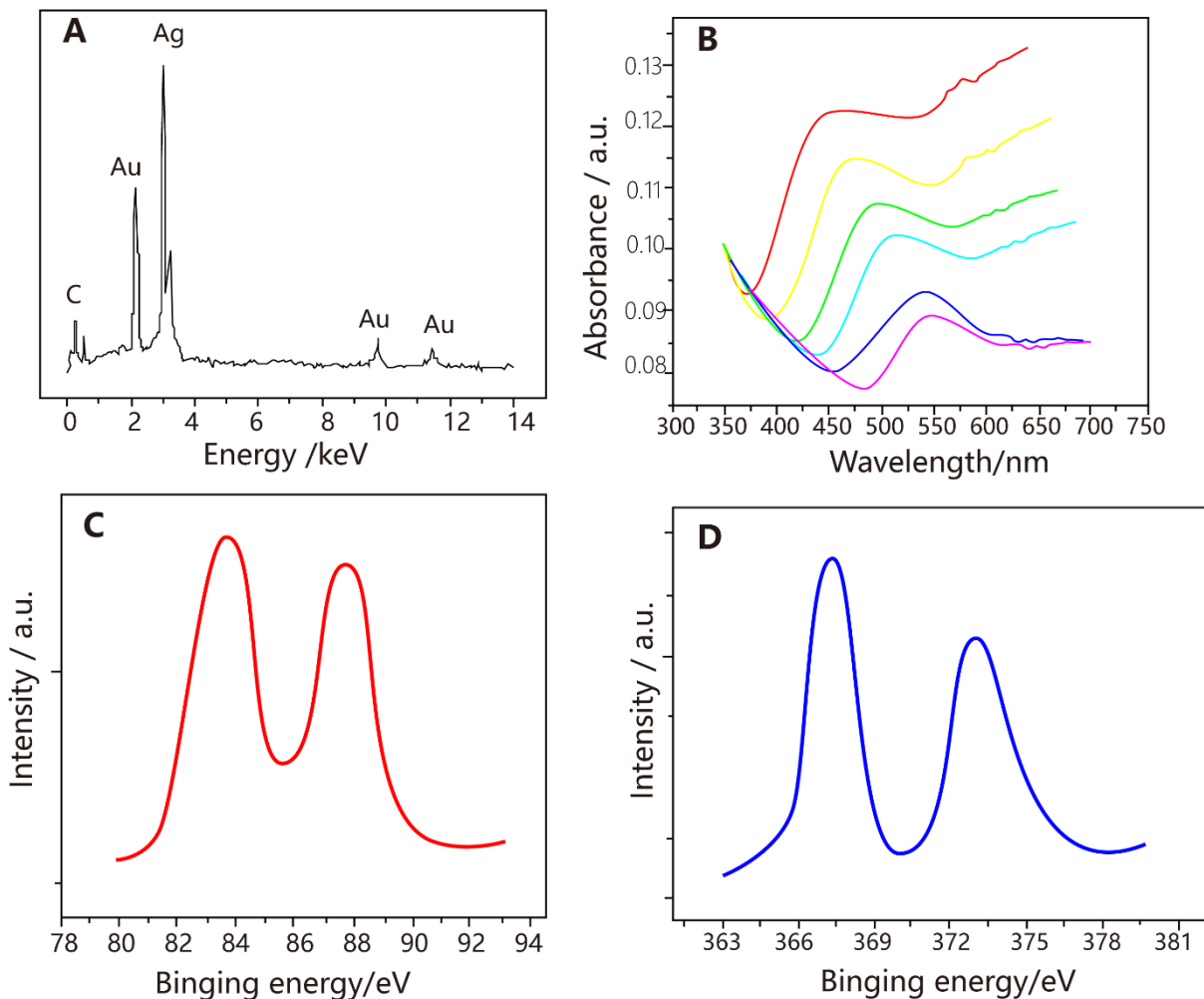


**Figure 1.** (A) EDX profile of Au–Ag alloy nanoparticles on GCE. (B) UVS absorption spectra of Au–Ag alloy nanoparticles with varying reaction time. (C) Au 4f and (D) Ag 3d core-level spectra obtained for drop-coated Au–Ag alloy nanoparticles

The chemical measurement of a drop-coated film of Au–Ag alloy NPs was performed using XPS, as indicated in Fig. 1C and D. As shown in Fig. 1C, the Au 4f spectrum was composed of two spin–orbit sections. The Au 4f<sub>5/2</sub> and 4f<sub>7/2</sub> peaks were observed at binding energy (BE) values of 87.7 eV and 84.1 eV, respectively, and are assigned to metallic Au [12]. As indicated in Fig. 1D, the Ag 3d spectrum consisted of two spin–orbit sections. The Ag 3d<sub>3/2</sub> and 3d<sub>5/2</sub> peaks were observed at BE values of 373.4 eV and 367.4 eV, respectively, and correspond to metallic silver [14]. The above results showed the presence of only one Ag and one Au form in solution, namely, Au<sup>0</sup> and Ag<sup>0</sup>. Based

on the XPS analysis, all the silver and gold ions involved in the synthesis of the nanoparticles were reduced and were in the metallic form.

Fig. 2A shows the electron transfer kinetics of a redox probe  $[\text{Fe}(\text{CN})_6]^{3-/4-}$  of varying electrodes using EIS measurements. The electron-transfer resistances of the redox processes of the probe obtained for the original GCE and the CDA-modified GCE, whereas those of the CDA/AuNP-modified GCE and the CDA/AgNP-modified GCE were lower. In addition, the lowest resistance of the redox process of the probe was observed for the CDA/Au–AgNP-modified GCE, suggesting that the remarkable electric conduction of the Au–Ag alloy NPs could promote electron transfer.

Different electrodes were characterized in 5 mM  $[\text{Fe}(\text{CN})_6]^{3-/4-}$  + 0.1 M KCl at 100 mV/s via CVs, as shown in Fig. 2B. It can be seen that the original GCE and the CDA-modified GCE each showed two pairs of well-defined redox peaks since  $\text{Fe}(\text{CN})_6^{3-/4-}$  exhibited reversible one-electron redox performance. A lightly accelerated interfacial charge transfer between the electrode and  $\text{Fe}(\text{CN})_6^{3-/4-}$  is observed for the CDA/AgNP/GCE and greatly increased redox peak currents are observed for the CDA/AuNP/GCE. The largest redox peak currents for  $\text{Fe}(\text{CN})_6^{3-/4-}$  were observed for our proposed GCE, which suggested the involvement of the Au–Ag alloy NPs in the increase in electroactive surface area. This involvement might have been because the Au–Ag alloy NPs possessed a large special surface area and desirable conductivity. The above results were consistent with the results of the EIS measurement.

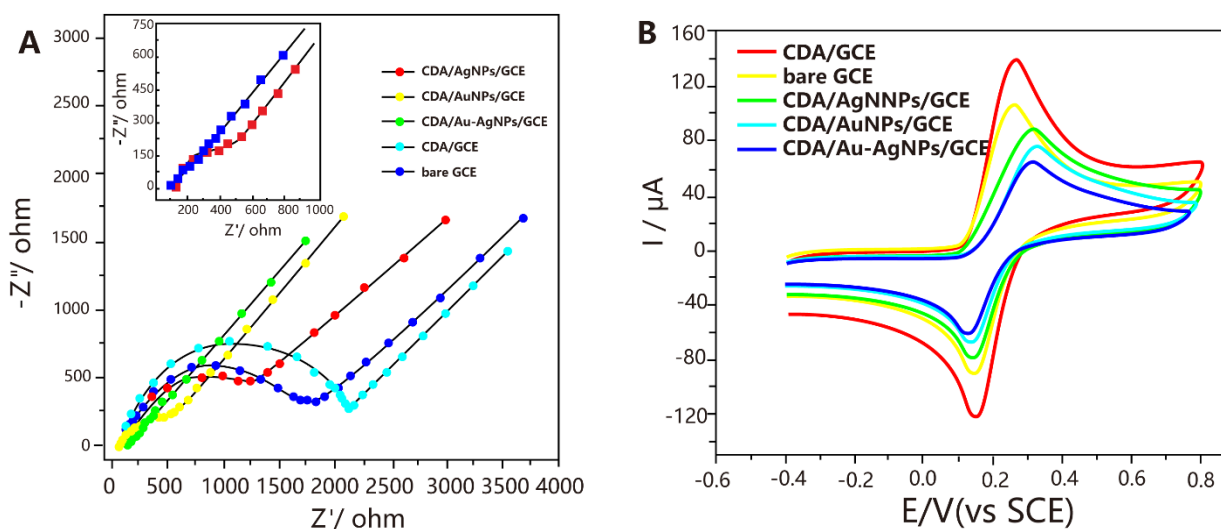


**Figure 2.** (A) Dependence of electrochemical impedance spectra of varying electrodes in 5 mM  $[\text{Fe}(\text{CN})_6]^{3-/4-}$  + 0.1 M KCl solution and (B) CVs of varying electrodes in 5 mM  $[\text{Fe}(\text{CN})_6]^{3-/4-}$  + 0.1 M KCl at 100 mV/s.

CV measurements were performed to study the electrochemical responses of paracetamol at varying electrodes. Only the original GCE exhibited an irreversible oxidation peak for paracetamol (Fig. 3A). However, a pair of well-defined redox peaks was observed for the Au–AgNP-modified GCE, associated with the reduction (0.35 V) and oxidation (0.40 V) of paracetamol. In addition, upon the modification of the bare GCE by CDA/Au–AgNPs, an obvious increase in the current responses of

this pair of well-defined redox peaks for paracetamol was observed, and a certain degree of increase in the background current of the CDA/Au–AgNP/GCE was also observed.

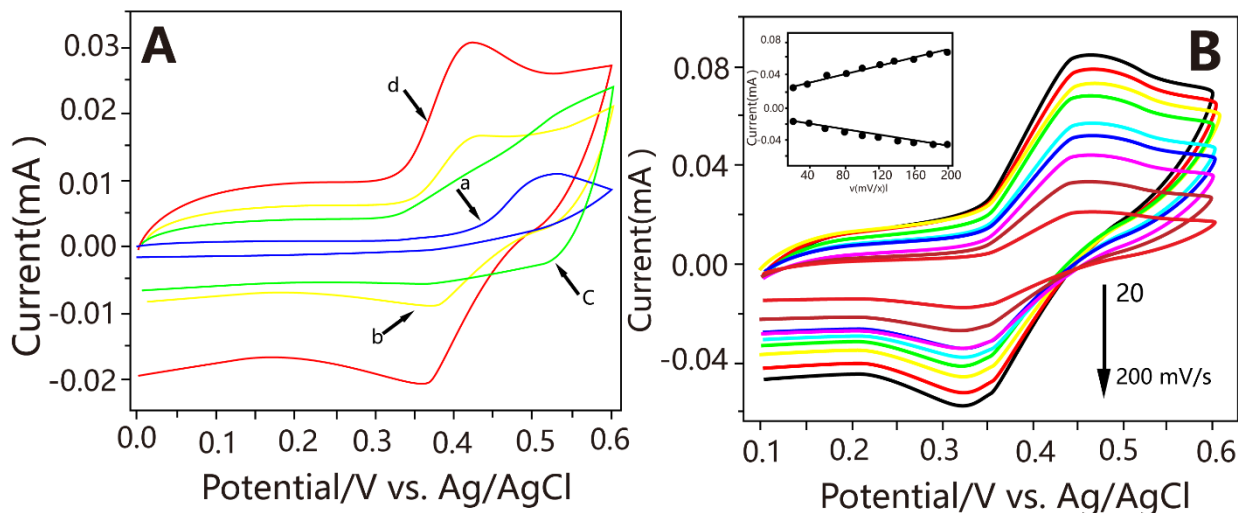


**Figure 3** (A) CVs of (a) the original GCE, (b) the Au–AgNP/GCE and (d) the CDA/Au–AgNP/GCE in PBS solution (0.2 M, pH 7.0) after adding paracetamol (0.1 mM) and of (c) the CDA/Au–AgNP/GCE before adding paracetamol at a scan rate of 50 mV/s. B) CVs of CDA/Au–AgNP/GCE in paracetamol (0.1 mM) (scan rate range: 20 - 200 mV/s). Corresponding plots of current responses vs scan rate are shown in inset.

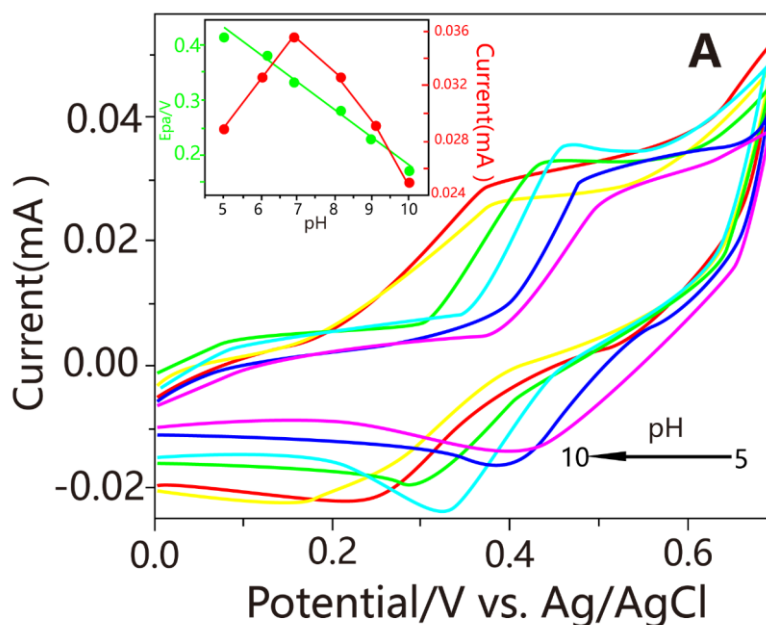


**Figure 4.** CVs of paracetamol (0.1 mM) at CDA/Au–AgNP/GCE in PBS solution (0.2 M) with varying pH: 5.0, 6.0, 7.0, 8.0, 9.0, 10.0 at a scan rate of 50 mV/s. The black line and blue line in the inset show the relationship between  $E_{pa}$  and pH and the effect of pH on the oxidation peak currents, respectively.

Fig. 3B shows the effect of scan rate on the redox current of paracetamol at the CDA/Au–AgNP/GCE. It can be seen that the scan rate increase led to an increase in the anodic and cathodic peak currents and to enlarged peak separation. In addition, as indicated in the inset of Fig. 3B, the anodic and cathodic peak currents were found to be linearly related to the scan rate (20 - 200 mV/s), revealing the adsorption-controlled property of the reaction of paracetamol at the  $\beta$ -CD/RGO/GCE [46, 47]. Moreover, the results indicate that two electrons are involved in the electrochemical redox process of paracetamol [48].

The effect of pH values on the redox performance of paracetamol at the CDA/Au–AgNP/GCE was studied via CV, as shown in Fig. 4. An obvious negative shift in the oxidation and reduction potentials was observed as the pH value increased, indicating the involvement of proton transfer in the electrochemical reaction of paracetamol [40, 46]. In addition, the oxidation potentials were found to be linearly related to the variation in pH, as shown by the black line in the inset in Fig. 6A. According to the Nernst equation, the slope value (0.053 V/pH) was nearly equivalent to the theoretical value (0.059 V/pH) [40, 43], suggesting the involvement of the same proportion of electrons and protons in the redox process.

Fig. 5A displayed the amperometric response of our proposed electrode after the successive adding paracetamol into PBS at pH 7.0. It can be clearly seen that changes in the concentration of paracetamol led to a quick response from our proposed electrode. A stable current was observed within 7 s after paracetamol addition. The calibration profile between the paracetamol concentrations (0.01 - 0.1 mM) and the current response is shown in the inset (Fig. 5A). The LOD was found to be 2.6  $\mu$ M (S/N = 3). As shown in Table 1, the LOD of the CDA/Au–AgNP-modified GCE was lower compared with that of several previously proposed electrodes, indicating that the CDA/Au–AgNP-modified GCE is applicable to paracetamol determination.

Moreover, the obtained CDA/Au–AgNP-modified GCE was utilized to analyse the amounts of paracetamol in three tablet samples collected from cultivated land as real drug samples. The results of the paracetamol content determination in these three tablet samples are shown in Table 2. As shown, the CDA/Au–AgNP-modified GCE had excellent performance in paracetamol detection in the drug samples.

We also investigated the effect of possible interfering agents on the electrochemical performance of paracetamol. The amperometric response of the CDA/Au–AgNP-modified GCE in the presence of paracetamol after adding varying interfering agents such as glucose, ascorbic acid, dopamine and uric acid is shown in Fig. 5B. A quick current response was observed after adding paracetamol (0.01 mM), whereas no variation in current response was observed after adding glucose, ascorbic acid, dopamine and uric acid (0.1 mM), indicating the remarkable selectivity of our proposed electrode even in the presence of interfering agents at 10-fold concentration.

I also investigated the effect of possible interfering agents on the electrochemical performance of paracetamol. The amperometric response of CDA/Au–AgNPs modified GCE in the presence of paracetamol after adding varying interferences such as glucose, ascorbic acid, dopamine and uric acid was shown in Fig. 5B. A quick current response was observed after adding paracetamol (0.01 mM), whereas the no variation in current response was observed after adding glucose, ascorbic acid,

dopamine and uric acid (0.1 mM), indicating the remarkable selectivity of our proposed electrode even in the presence of interfering agents at 10-fold concentration.

**Table 1.** Comparison of varying electrodes toward the paracetamol detection.

Electrode	Linear range (mM)	Detection of limit ( $\mu\text{M}$ )	Reference
Single-Walled Carbon Nanotube/ZnO	0.01–0.09	0.077	[49]
Printex 6L Carbon Nanoballs	0.08-0.23	0.056	[50]
ERGO/ZrO <sub>2</sub>	0.03-0.174	—	[51]
$\beta$ -cyclodextrin functionalizedRGO	0.01-0.8	2.3	[52]
Pd/GO	0.05-0.5	0.0022	[53]
MWCNTs and a G4.0 PAMAM modified GCE	0.0003-0.2	0.0001	[54]
CDA/Au–AgNPs modified GCE	0.01-0.1	2.6	This work

**Table 2.** The contents and recoveries of CDA/Au–AgNPs modified GCE for paracetamol determination in tablet (n=3).

Sample	Found (mM)	Added (mM)	Found ( $\mu\text{M}$ )	Recovery (%)	RSD (%)
1	0.142	0.10	0.246	101.65	3.21
2	0.141	0.20	0.331	97.07	2.55
3	0.137	0.30	0.429	98.17	0.96

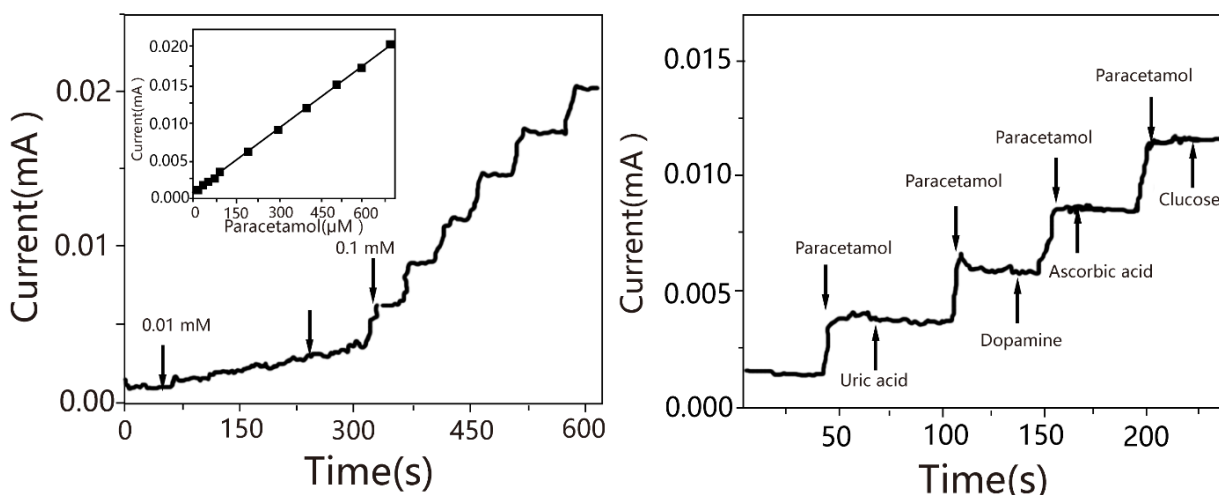


**Figure 5** (A) Characteristic current-time response of CDA/Au–AgNP-modified GCE upon the successive addition of paracetamol at 0.01 mM and 0.1 mM. (B) Amperometric response of CDA/Au–AgNP/GCE upon the addition of paracetamol, uric acid, dopamine, ascorbic acid and glucose (0.1 mM) in PBS solution.

#### 4. CONCLUSIONS

This study proposed the fabrication of a CDA/Au–AgNP-modified GCE and used it as a paracetamol electrochemical sensor for the first time. The proposed sensor inherited the merits of Au–AgNP materials and CDA, thus leading to substantial enhancement in the electrochemical performance in response to paracetamol. To be specific, the proposed sensor displayed an acceptable linear detection range (0.01 - 0.1 mM) and a low LOD (2.6  $\mu$ M). In addition, the anti-interference performance of our newly developed paracetamol sensor was confirmed to be remarkable.

#### References

1. N. Toshima and T. Yonezawa, *New J Chem*, 22 (1998) 1179.
2. S. Link, Z. Wang and M. El-Sayed, *J Phys Chem B*, 103 (1999) 3529.
3. M. Mallin and C. Murphy, *Nano Letters*, 2 (2002) 1235.
4. S. Liu and M. Han, *Adv Funct Mater*, 15 (2005) 961.
5. J. Fernández, D. Walsh and A. Bard, *Journal of the American Chemical Society*, 127 (2005) 357.
6. R. Ferrando, J. Jellinek and R. Johnston, *Chemical Reviews*, 108 (2008) 845.
7. S. Gurmen, B. Ebin, S. Stopić and B. Friedrich, *J. Alloy. Compd.*, 480 (2009) 529.
8. C. Lee, Y. Cheng, H. Chang and D. Chen, *J. Alloy. Compd.*, 480 (2009) 674.
9. M. Brust, M. Walker, D. Bethell, D.J. Schiffrin and R. Whyman, *Journal of the Chemical Society, Chemical Communications*, (1994) 801.
10. P. Mulvaney, M. Giersig and A. Henglein, *The Journal of Physical Chemistry*, 97 (1993) 7061.
11. M. Gericke and A. Pinches, *Hydrometallurgy*, 83 (2006) 132.
12. A. Ahmad, P. Mukherjee, S. Senapati, D. Mandal, M. Khan, R. Kumar and M. Sastry, *Colloids and surfaces B: Biointerfaces*, 28 (2003) 313.
13. P. Mukherjee, S. Senapati, D. Mandal, A. Ahmad, M. Khan, R. Kumar and M. Sastry, *ChemBioChem*, 3 (2002) 461.
14. S. Senapati, A. Ahmad, M. Khan, M. Sastry and R. Kumar, *Small*, 1 (2005) 517.
15. I. Milošev and M. Remškar, *Journal of Biomedical Materials Research Part A*, 91 (2009) 1100.
16. B. Reiss, C. Mao, D. Solis, K. Ryan, T. Thomson and A. Belcher, *Nano Letters*, 4 (2004) 1127.
17. K. Aslan, S. Malyn and C. Geddes, *Journal of the American Chemical Society*, 128 (2006) 13372.
18. Q. Kang, L. Yang and Q. Cai, *Bioelectrochemistry*, 74 (2008) 62.
19. S. Guo, S. Dong and E. Wang, *J Phys Chem C*, 112 (2008) 2389.
20. N. Toshima, T. Yonezawa and K. Kushihashi, *Journal of the Chemical Society, Faraday Transactions*, 89 (1993) 2537.
21. N. Kariuki, J. Luo, M.M. Maye, S. Hassan, T. Menard, H. Naslund, Y. Lin, C. Wang, M. Engelhard and C. Zhong, *Langmuir*, 20 (2004) 11240.
22. S. Zhou, K. McIlwrath, G. Jackson and B. Eichhorn, *Journal of the American Chemical Society*, 128 (2006) 1780.
23. J. Huang, W. Hwang, Y. Weng and T. Chou, *Thin Solid Films*, 516 (2008) 5210.
24. H. Cui, J. Ye, W. Zhang, C. Li, J. Luong and F. Sheu, *Anal. Chim. Acta.*, 594 (2007) 175.
25. X. Zhu, G. Kang and X. Lin, *Microchim. Acta.*, 159 (2007) 141.
26. A. Pal, S. Shah and S. Devi, *Colloids and Surfaces A: Physicochemical and Engineering Aspects*, 302 (2007) 51.
27. R. Goyal, V. Gupta, M. Oyama and N. Bachheti, *Electrochemistry Communications*, 7 (2005) 803.
28. P. Chandra, N. Son, H. Noh, R. Goyal and Y. Shim, *Biosensors and Bioelectronics*, 39 (2013) 139.
29. K. Heard, *N. Engl. J. Med.*, 359 (2008) 285.
30. K. Blake, D. Bailey, G. Zientek and L. Hendeles, *Clinical Pharmacy*, 7 (1988) 391.

31. H. Toklu, A. Şehirli, A. Velioglu-Ögünç, Ş. Çetinel and G. Şener, *European Journal of Pharmacology*, 543 (2006) 133.
32. Sirajuddin, A. Khaskheli, A. Shah, M. Bhangar, A. Niaz and S. Mahesar, *Spectrochimica Acta. Part A, Molecular and Biomolecular Spectroscopy*, 68 (2007) 747.
33. J. Vilchez, R. Blanc, R. Avidad and A. Navalón, *Journal of Pharmaceutical and Biomedical Analysis*, 13 (1995) 1119.
34. A. Abu-Qare and M. Abou-Donia, *Journal of Pharmaceutical and Biomedical Analysis*, 26 (2001) 939.
35. K. Kumar and R. Letha, *Journal of Pharmaceutical and Biomedical Analysis*, 15 (1997) 1725.
36. D. Easwaramoorthy, Y.-C. Yu and H.-J. Huang, *Anal. Chim. Acta.*, 439 (2001) 95.
37. A. Trettin, A. Zoerner, A. Böhmer, F. Gutzki, D. Stichtenoth, J. Jordan and D. Tsikas, *Journal of Chromatography B*, 879 (2011) 2274.
38. A. Kunkel, S. Günter and H. Wätzig, *ELECTROPHORESIS*, 18 (1997) 1882.
39. Y. Li, S. Feng, S. Li, Y. Zhang and Y. Zhong, *Sensors and Actuators B: Chemical*, 190 (2014) 999.
40. A. Kutluay and M. Aslanoglu, *Sensors and Actuators B: Chemical*, 185 (2013) 398.
41. N. Tzierkezos, S. Othman and U. Ritter, *Ionics*, 19 (2013) 1897.
42. M. Zheng, F. Gao, Q. Wang, X. Cai, S. Jiang, L. Huang and F. Gao, *Materials Science & Engineering. C, Materials for Biological Applications*, 33 (2013) 1514.
43. W. Si, W. Lei, Z. Han, Y. Zhang, Q. Hao and M. Xia, *Sensors and Actuators B: Chemical*, 193 (2014) 823.
44. C. Kung, C. Lin, R. Vittal and K. Ho, *Sensors and Actuators B: Chemical*, 182 (2013) 429.
45. S. Mandal, P. Selvakannan, R. Pasricha and M. Sastry, *Journal of the American Chemical Society*, 125 (2003) 8440.
46. J. Li, J. Liu, G. Tan, J. Jiang, S. Peng, M. Deng, D. Qian, Y. Feng and Y. Liu, *Biosensors & Bioelectronics*, 54 (2014) 468.
47. M. Devaraj, R. Deivasigamani and S. Jayadevan, *Analytical Methods*, 5 (2013) 3503.
48. L. Fu, G. Chen, N. Jiang, J. Yu, C. Lin and A. Yu, *Journal of Materials Chemistry A*, 4 (2016) 19107.
49. K. Ngai, W. Tan, Z. Zainal, R. Zawawi and J. Juan, *Science of Advanced Materials*, 8 (2016) 788.
50. P. Raymundo-Pereira, A. Campos, C. Mendonça, M. Calegari, S. Machado and O. Oliveira Jr, *Sensors and Actuators B: Chemical*, 252 (2017) 165.
51. A. Ezhil Vilian, M. Rajkumar and S. Chen, *Colloids and Surfaces B: Biointerfaces*, 115 (2014) 295.
52. L. Fu, G. Lai and A. Yu, *RSC Advances*, 5 (2015) 76973.
53. J. Li, J. Liu, G. Tan, J. Jiang, S. Peng, M. Deng, D. Qian, Y. Feng and Y. Liu, *Biosensors and Bioelectronics*, 54 (2014) 468.
54. Y. Zhang, X. Liu, L. Li, Z. Guo, Z. Xue and X. Lu, *Analytical Methods*, 8 (2016) 2218.